# DEVELOPMENT OF A LEAN PRODUCTION PROCESS FOR A THERMOPLASTIC COMPOSITE UPPER STAGE PROPELLANT TANK

Lars Brandt, Dominik Deden, Fabian Bruckner, Manuel Engelschall, Monika Mayer, Alfons Schuster, Dorothea Nieberl, Christoph Frommel, Florian Krebs, Stefan Jarka, Frederic Fischer, Lars Larsen
German Aerospace Center (DLR), Center for Lightweight Production Technology (ZLP)
Am Technologiezentrum 4
Augsburg 86159

## ABSTRACT

Private space flight disrupted the international launcher industry with an innovative spirit, tremendous funding and the objective to provide low cost access to space. In order to stay a relevant competitor the European launcher industry has to increase its launchers performance while reducing the manufacturing costs. The Center for Lightweight Production Technology (ZLP) of the German Aerospace Center (DLR) in Augsburg developed an innovative and data driven manufacturing process for a liquid hydrogen propellant tank. To account for the complex interior of the tank (e.g. fill level indicators and propellant management devices ) an integral design with thermoplastic CFRP LM-PAEK material was developed. Components were manufactured individually in an automated fiber placement (AFP) process and subsequently assembled by ultrasonic welding. This allows a reduction of complexity in individual parts and ensures easy installation of systems inside the tank. Throughout manufacturing inline quality assurance methods are used, the data is coupled with machine parameters and automatically evaluated. The paper gives an overview of the design approach, processes and methods to manufacture a scaled propellant tank demonstrator.

## 1. INTRODUCTION

The entrance of commercial providers into the mostly institutionalized launcher market reduces costs of space transportation significantly, whereby global competition and the need for innovation increases. In order to compete in these new market conditions European launcher systems face the challenge of reducing production costs while increasing performance of their launchers. An effective approach is the utilization of high-performance materials such as CFRPs combined with a focus on lean production processes for new launcher parts. Especially the reduction of structural weight in the upper stage, which passes all flight phases, has a significant impact on performance. The reduction of mass in these components is equal to the increase in payload capacity.

## 2. STATE OF THE ART

Development of composite cryogenic tanks began in 1987 in the US when McDonell Douglas developed a liquid hydrogen (LH2) tank. The tank is cylindrical shaped with a diameter of 2.4 m and a length of 4.88 mm. It was manufactured with AFP based on a pre-impregnated epoxy resin CFRP. Thermal cycling of the tank, which means filling and draining of the propellant, was successful. The first flying composite tank DC-XA was used to store LH2 and liquid oxygen (LOX). It consists of two epoxy CFRP components with a diameter of 2.4 m and is equipped with an internal insulation. The two parts where bonded with a belly-band joint. Its

successor the LM-X33 is complexly shaped with a honeycomb core made out of thermoset CFRP. During pressurizing with LH2 the outer skin delaminated. Northrup Grumman built a 1.8 m x 4.6 m improvement to the LM-X33 with a vented honeycomb and an additional permeation barrier. To prevent microcracking thin prepreg epoxy CFRP has been used. In 2014 NASA developed and built full-scale LH2/LOX tanks. The cylindrical part has a diameter of 5.5 m and a length of 5.96 m. It was produced with prepreg, epoxy CFRP and various co-curing cycles. Although mechanical as well as thermal cycling tests were successful, it was not deployed in current launcher developments.[1, 6, 13] Space X manufactured a LOX tank with a diameter of 12 m, even though it passed a first pressure test its reported that development is discontinued [7, 13].
For its Electron Launcher RocketLab developed a composite LOX tank but no further details are published [9].
Sippel et. al [10] investigated four subscale composite cryogenic tanks in the European project Cryogenic Hypersonic Advanced Tank Technologies (CHATT). They designed several cylindrical shaped tanks with and without liner as well as a complexly shaped tank. The most promising concept was a liner-less concept tested in a pipe shape. DLR manufactured a combination of glass and carbon fiber reinforced epoxy with a diameter of 2.4 m and 3 m in length. Several smaller cryogenic thermoset CFRP tanks are reported in [2] the largest being a tank produced by Mitsubishi Heavy industries with a diameter of 1 m and 1.7 m in length with a honeycomb structure.

Current LH2 propellant tanks are mostly based on thermoset epoxies, partly supplemented by additives to enhance thermal performance. They are designed monolithic with exceptions being joined with a belly band or co-cured. DLR envisions a composite tank that is divided into two separate parts for easy inspection and systems equipment. With the use of thermoplastic LM-PAEK its benefits of high toughness, good thermal and chemical resistance is utilized. The use of thermoplastic enables the usage of lean manufacturing processes such as AFP and thermoplastic welding. For the AFP a novel flash lamp heating system is deployed and an innovative welding technology, continuous ultrasonic welding, is used to join and seal the two parts of the tank.
In order to ensure the high safety standards of a part as critical as a propellant tank, strong quality assurance measures are taken. This is a main cost driver in production of tanks. The issue of costly 100% inspection is addressed with two innovative inline quality assurance methods: the tape profile sensor system and inline thermography. All data is acquired and evaluated to ensure quality. The following chapters will show the design approach, explain the manufacturing and quality processes and show the results for the demonstration build.

## 3. PROPELLANT TANK DESIGN

Figure 1 depicts the developed design. The part has a diameter of 1.3 m and length of 2 m. The dome including the nozzle adapter is indicated in red. Blue is the integral component with two skirts, the lateral surface and the second dome. The dome is equipped with a generic propellant management system that serves various functions: it prevents propellant to slosh, guides it to the nozzle opening and additionally acts as counterholder for the welding process. In the case of this manufacturing demonstrator the systems components are completed in aluminum. The adaption to CFRP can be done easily preventing thermal expansion problems and facilitate welding onto the skin.
The nozzle adapter and flange lid are two identically designed aluminum parts. The inner section is bonded to the LM-PAEK domes. Between the outer and inner flange sealing material

is applied and the parts are bolted together. Thus the CFRP dome is crimped between the flange parts.

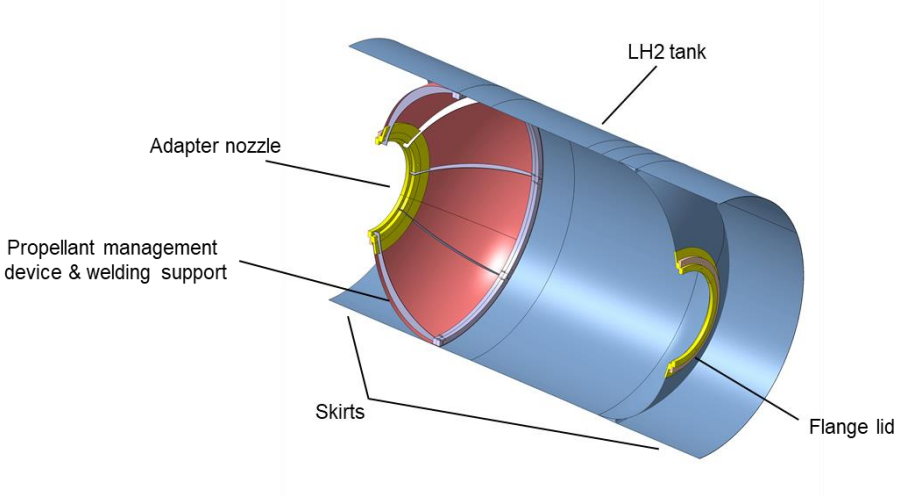


**Figure 1: DLR design for a cryogenic LH2 tank**

The laminate stacking sequence of the tank was evaluated by modelling of different static and buckling load cases considering a temperature of 20 K and a pressure of 5 bars. While for the domes and the tank itself, a stacking of eleven plies, resulting in a thickness of 1.54 mm was sufficient. In the skirts area 16 layers of 0° and 90° plies where used to eliminate buckling in these areas. The additional reinforcement skirt layers are designed to have an overlap of at least 210 mm. This results in a total laminate thickness of 2.38 mm in the skirts. The 0° fiber orientation in this case is defined along the rotational axis of the tank structure. The thickness of one consolidated layer of the used CF/LM-PAEK tape was measured to be 0.14 mm.

## 4. MANUFACTURING PROCESS

For the production of the tank several production technologies developed at the ZLP have been deployed. First, the parted structure of the tank is built in an in-situ automated fiber placement (AFP) process with flashlamp heating. In a second step the different sub-parts are joined by thermoplastic welding using a continuous ultrasonic welding process. The manufacturing process is displayed in Figure 2.

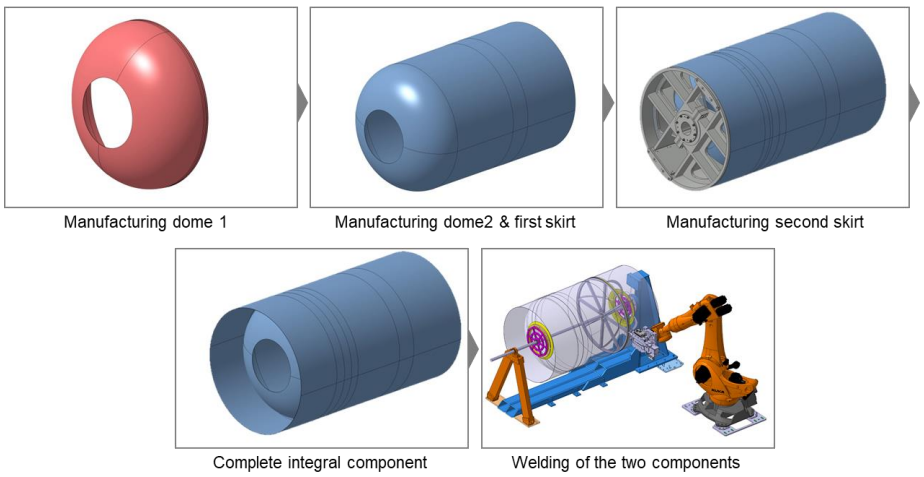


**Figure 2: Manufacturing process**

The main tank structure on the left is placed directly on the tool. Subsequently a skirt tooling is installed over the placed structure in order to add the skirt displayed in the center. The skirt is consolidated directly onto the tank, forming a single part. Lastly, the dome in the right picture is produced onto the plane tooling. The two parts are then assembled and joined by continuous ultrasonic welding.

### 4.1 In-situ Flashlamp Automated Fiber Placement (F-AFP)

AFP is a well-established manufacturing process for CFRP components of low to medium complexity. A various number of narrow prepreg tapes from spools is placed on a surface with a roller that applies compaction pressure. The incoming tapes are heated to processing temperatures, typically by laser heating. In our case the heat source used is a pulsed high energy xenon flashlamp. Flashlamps are an alternative to lasers that may show potential advantages for the process such as reduced safety measures.

The lay-up head used is the MTLH manufactured by AFPT and was originally designed for laser heating. The head was adopted for the use with a flashlamp. It can process three ½" tapes of various thermoplastics. The endeffector is mounted on a six axis industrial robot on a linear axis. The setup is capable of the production of rotational parts of up to 4 m length and a diameter of up to 3 m. So far PPS and LM-PAEK have been processed successfully. The main difference between laser- and flashlamp-heating is the spectrum in which both lamps operate. A laser is a monochromatic lightsource that emits a single frequency often in the range of 1090 nm. A flashlamp emits a broadband spectrum from 350 to 1090 nm. Therefore the absorption of energy in the material is fundamentally different for both heat sources. The differences for the mechanical properties are currently investigated in a comparison study with an identical laser setup.

LM-PAEK can be manufactured at a speed of 70 mm/s with our current flashlamp system. The material is typically placed directly on an unheated tooling. If placed on an unheated tooling the crystallinity is below 7% due to the high cool down rate. With a subsequent tempering cycle the crystallinity can be increased up to 35% which also increases mechanical properties. However thermal warpage may cause inner stresses ultimately weakening the overall structure. The benefits of a two stage process are currently under investigation. Our most recent study showed that specimen placed at optimal process parameters had a shear strength of 26.7 MPa if untreated compared to 35.9 MPa if annealed.

### 4.2 Continuous Ultrasonic Welding for a Curved Circumferential Seam

The assembly of the two individual parts of the tank is done by continuous ultrasonic welding, handled by a robotic manipulator. With this setup the applications of welding circular bonds is possible in several sequential welds. By utilization of an additional rotational axis circumferential welds with 360° can be achieved.

The ultrasonic welding process directs an orthogonal vibration into the composite laminates. In the boundary layer between the joining partners the energy director made of pure polymer matrix provides increases vibration damping and friction, which leads to the desired melting in this depth level.[11, 12] Amplitude, frequency and welding pressure determine the amount of energy input. In a conventional static welding process the duration of the exposure is defined via the time setting. Here it is the speed of overrun, simply called welding speed. It determines the local energy input, the cooling time under pressure and ultimately the cycle time of the

joining task.[8] Figure 3 depicts the experimental setup, already tested on long and curved weld lines.

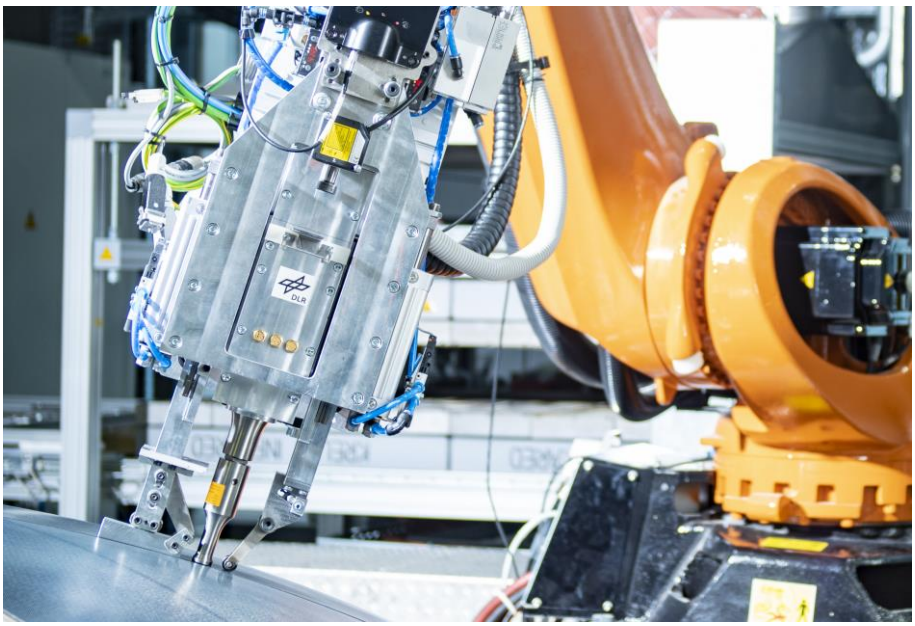

**Figure 3: continuous ultrasonic welding process for joining long and not just straightforward appeared weld lines**

Thanks to a function-integrated lightweight construction, the required propellant management device of the container fulfills the tasks of stabilization the fuel on the one hand, through its specially designed ribs. On the other hand this structure works as the ultrasonic weld anvil, necessary for the joining process.

The welding infrastructure is a Branson DCXs 20VRT generator with a peak output power of 4 kW and a constant frequency of 20 kHz. The robot manipulator is a high accuracy KUKA Quantec KR210 R3100, able to handle the tool weight and process forces acting out of the system. Experiments are carried out with peak to peak amplitude of 95 % of the maximum adjustable value, a welding pressure in the range of 400 to 600 N and a welding speed of 20 to 25 mm/s. The sonotrode diameter of the spherical bearing surface is 25 mm. The weld seam shaping is a triple parallel design with a target width of 25 mm each, in a simple overlap with a semi-finished attached width of approximately 100 mm.

Specific challenges are the curved circumferential seam, the irregular surfaces of the non-tooling side of sub-parts inherent to the AFP process and the impossible provision of a welding path caused by the circular design.

## 5. INLINE QUALITY ASSURANCE

To assess the quality of tape positioning and in-situ consolidation several inline quality assurance systems were considered. A tape profile sensor (TPS) detects gaps, twists, overlaps or missing tows. Inline thermography is used to evaluate cooling rates and consolidation. Additionally gaps, overlaps and missing tapes are detectable [3]. Both systems aim to detect deviations from process parameters and production tolerances as soon as possible to avoid costly rejects and improve reparability.

## 5.1 Tape profile sensor (TPS)

A tape profile sensor (TPS) based upon a laser light sheet measurement setup is attached to the AFP-head. The TPS has a modular design in order to make it adaptable to different use cases. The system consists of a camera and a line laser. Both components, as shown in Figure 4, can be adjusted independently in order to enable the best possible illumination of the surface and therefore more accurate evaluation of the laser line. For our use case, a 45°/45°-light field measurement geometry yielded best results, since the tapes are highly reflective.

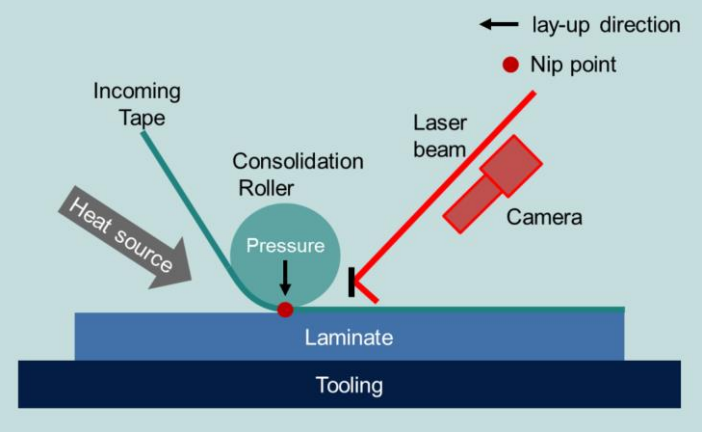


**Figure 4: Principle of T-AFP process with inspection system attached**

The TPS is triggered via an encoder input which is fed by the fast send driver of the KUKA robot. A discretized scanline is created per encoder tick (currently 0.1 mm). After elimination of erroneous and outlying data the points are connected to obtain a height profile, which is then evaluated inline, allowing gaps, overlaps and missing tows to be detected (Figure 9). Having transformed the point coordinates from the TPS coordinate system to the component coordinate system, a point cloud compatible with the CAD data is generated. Since the point cloud is composed of a multitude of scanlines, the holistic evaluation can only be performed offline. With the help of meta information, like nominal values of the tape start position, early or late cuts can be detected.

## 5.2 Inline thermography

The thermography camera (Infratec HD Head 800) is mounted directly on the AFP head and measures the temperature of the tapes after compression with the compaction roller. The camera is equipped with a wide angle optic to measure the tapes starting near to the roller and wide enough to superimpose enough images for active thermography evaluation. With the help of Common Vision Blox (CVB) software and self-developed scripts in C++ the thermography camera control was established.

Conventional active thermography evaluation with Fourier transformation is conducted on a series of superimposed images recorded from a stationary point of view [5]. As the camera is non-stationary in this use case it is not possible to use this approach without modifications. Therefore a pixel tracking over a series of images will be established. The camera position relative to the substrate is needed to evaluate the pixel movement over time. The AFP head is mounted on a KUKA industrial robot. Its position can be recorded together with a timestamp and an active synchronization through KUKA fast send driver (FSD). These robot positions and timestamps are matched with the timestamps of the thermography measurement which assigns each frame of temperatures with a time and robot position.

## 5.3 Data

As described above real time data acquisition and evaluation are vital in demanding low volume production environments. Therefore we set up the tape laying process with an integrated data management system (IDMS) which allows capturing time series data as well as event-based data from all process participants. This includes the controllers of the tape laying head, the robot, the heating source and the overarching machine PLC as well as the quality assurance systems.

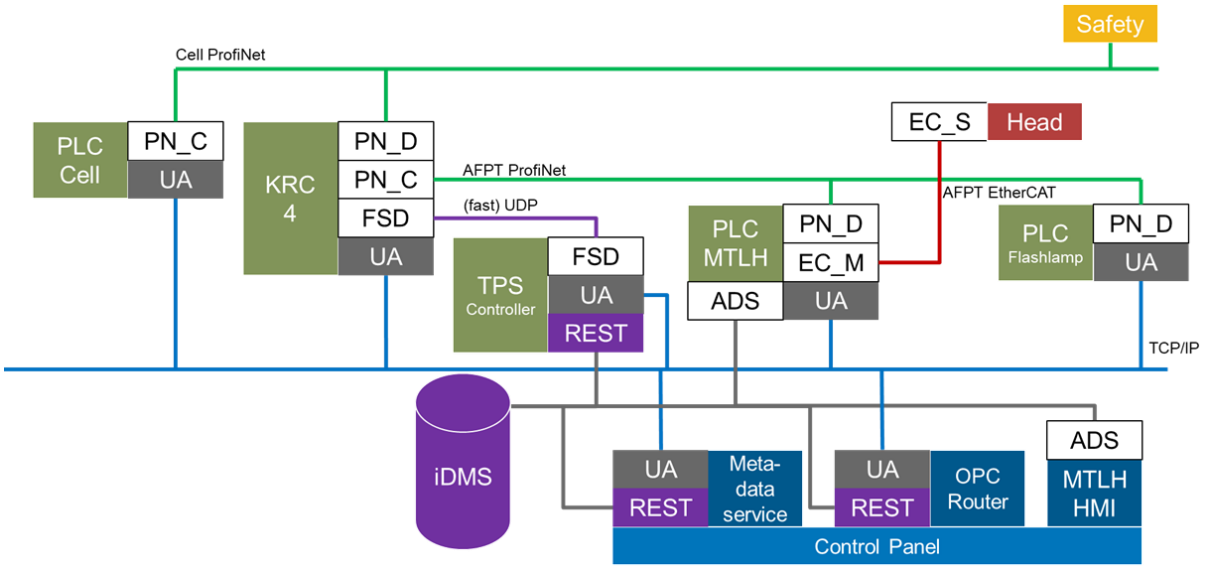


**Figure 5: Schematic overview of data collection system and interfaces**

In terms of data amount we capture roughly 1000 time series with varying frequency (250-10 Hz) depending on the data source's capability to supply data. All time series are exposed on the data providers through OPC UA servers [4]. To capture this data we use the proprietary industrial solution "OPC Router" which enables a robust and scalable collection of real time data as well as monitoring capabilities regarding data collection itself.

Regarding event-based data each system can also provide data on its own volition. This applies especially for image based data (e.g. the tape profile sensor) as this data is only available after a track has finished.

An intelligent context service infers metadata for annotation of collected data through observation of the machines states. All collected data is automatically annotated with this metadata to allow easy selection of relevant regions of interest in analysis regarding time of capture, layer and track number as well as spatial location on the part.

For real time monitoring we integrated "Grafana" as a dashboard provider to monitor process execution and identify emerging problems through trend analysis. For further analysis after production an analysis suite is developed. Its enabling a in depth analysis of process data dependencies as well as part quality estimation.

# 6. RESULTS

As described in paragraph 4 the demonstrators lay-up was planned to be done in three steps: The dome, the tank and the integral skirt, which is consolidated directly onto the placed main

structure of the tank. There are different challenges to every segment. The dome is placed only on the spherical part of the tool which makes the first ply adhesion difficult. The tank has the most layers with comparably long tracks and a 90° winding layer consisting of a single 113 m track. Finally the skirt includes a distinct change in diameter in the transition area between skirt and tank where in addition the skirt is consolidated directly onto the tank. In the following the production of each segment and the associated challenges are described.

## 6.1 Production of the demonstrator

The dome has a symmetric stacking with a layer sequencing of $[+60/-60/+30/-30/\pm\overline{45}]_s$. Due to collision between the endeffector and the tooling each ply angle is associated with a different pole diameter. Additionally the different pole diameters account for the material accumulation which is bound to occur if no tapes are dropped during the layup and help to generate a uniform thickness throughout the dome. ±60° layers end at a pole diameter of 550 mm, ±45° layers at 650 mm and ±30° layers at 750 mm. It was tested if tapes of the first ply could be fixed at the beginning and end of each track with adhesive heat resistant polyimid tape (kapton) which resulted in tape slippage in the double curvature areas of the part. A second trial tested first ply adhesion to be achieved by a layer of pure LM-PAEK matrix foil fixed by double sided kapton adhesive tape on which the CF\LM-PAEK tapes are placed. In the spherical part of the tool the matrix foil was shaped with heat to match the surface. This resulted in small wrinkles that influenced the tape position. In reaction to this the pure matrix foil was tailored in to smaller pieces as displayed in Figure 6 to fit the double curvature section of the part, assembled via ultrasonic weld spots. It allowed for an exact tape positioning without slippage.

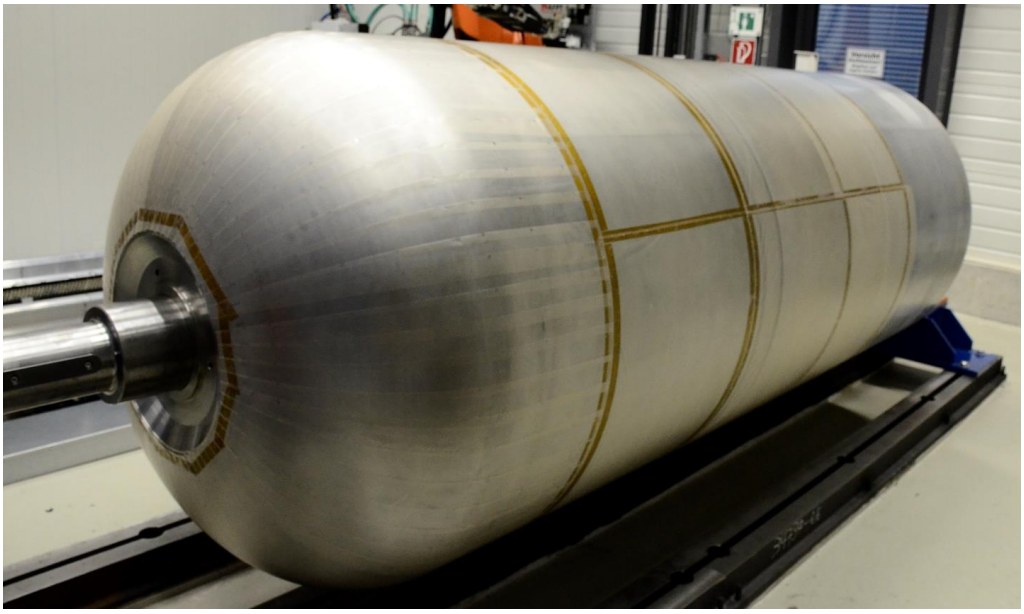

**Figure 6: LM-PAEK matrix foil for first ply adhesion tailored to fit the tooling**

The image shows the first ply adhesion layer applied to the entire tooling. The spherical area consists of 52 identically shaped matrix foil cutouts. The beginning and the end are fixed with double sided kapton adhesive tape. Utilizing this first ply concept the adhesion was sufficient to prevent slippage of the tape, though other defects associated with heavy steering were still observed. Most noticeable the placed tapes show a significant fold in as seen in Figure 7. The curvature of the dome increases to the pole opening resulting in a minimum steering radius of approximately 300 mm. At a steering radius of around 900 mm the tapes fold at the inner radius

and buckling of the tape is observed. This indicates that either steering radii need to be increased or the tape width needs to be decreased in future applications.

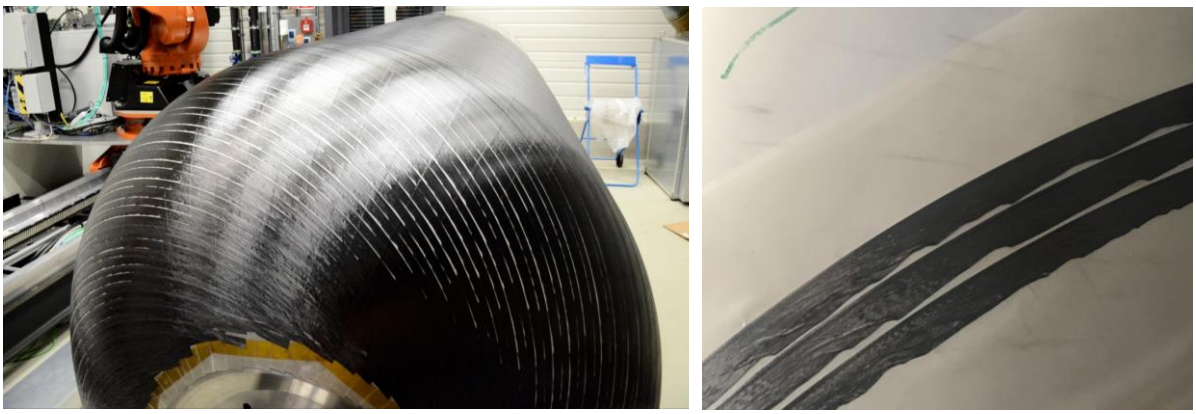

**Figure 7: Fold in defect in the first layer (60°) (left) and in detail (right)**

Manufacturing of the tank part showed problems due to the heat losses in the flashlamp system. While layup of longer tracks the lamp heats the layup head structure such as tape guides to unacceptable temperatures leading to sticking or degraded tapes. An air-cooled ceramic heat shield was installed to prevent degradation. However, these energy losses are not acceptable in an industrial application. If the energy is sufficiently directed into the material and distributed accordingly, faster process speeds can be expected. The integral part has been built with the same first layer design which proofed to be sufficient. Before the installation of the skirt tooling a 3D printed seam was placed between skirt and tank to support the gusset and moderate peeling forces. In this case polycarbonate (PC) parts were bonded the tank with adhesive two component epoxy. Printable LM-PAEK is available on the supplier market now and is to be used in future iterations. At the time of publication of this paper the skirt missed 10 additional layers to be fully completed. Due to the unfinished part the welding could not be shown in this paper. However, trials on individual 60° ring segments with the identical laminate structure as the tank showed promising results. At this stage the major challenges for the upscaling of the F-AFP process from small panels to a complex part have been the overheating of the endeffector in long track, the degaradtion of the silicone compaction unit and the small steering radii.

## 6.2 Inline quality assurance

The inline thermography system was integrated and tested during production of two samples. Pre-defined defects (pieces of kapton, aluminum and CFRP material) were inserted between layers of tape. Those defects are visible in the thermographic measurement as seen in Figure 8.

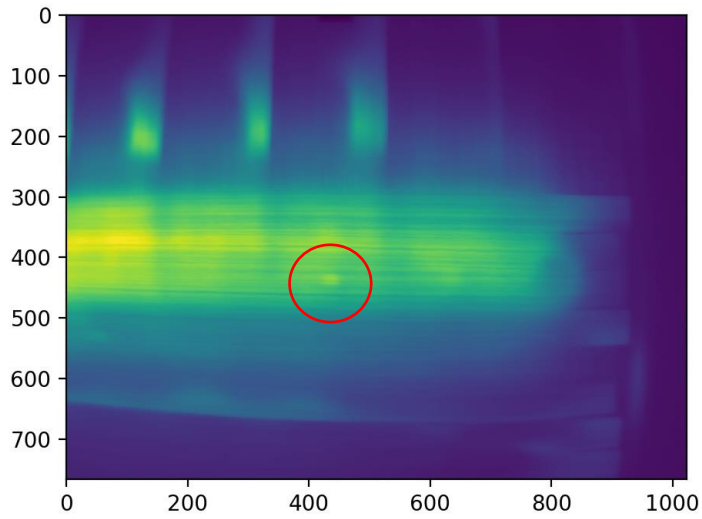


**Figure 8: Thermographic image of artificial defect (axes: position in pixel)**

The TPS was integrated in the tape laying head and tested during the layup of a test plate. Figure 9 (middle) shows the raw concatenated height profiles. On the right the inline evaluation of gaps, overlaps and tow borders is added to the scanlines. The 3D point cloud of the measured data is visualized on the left. Three scans are superimposed resulting in a higher point density in the overlapping parts in the middle. All measured data is automatically stored in a database with unique IDs to track the data.

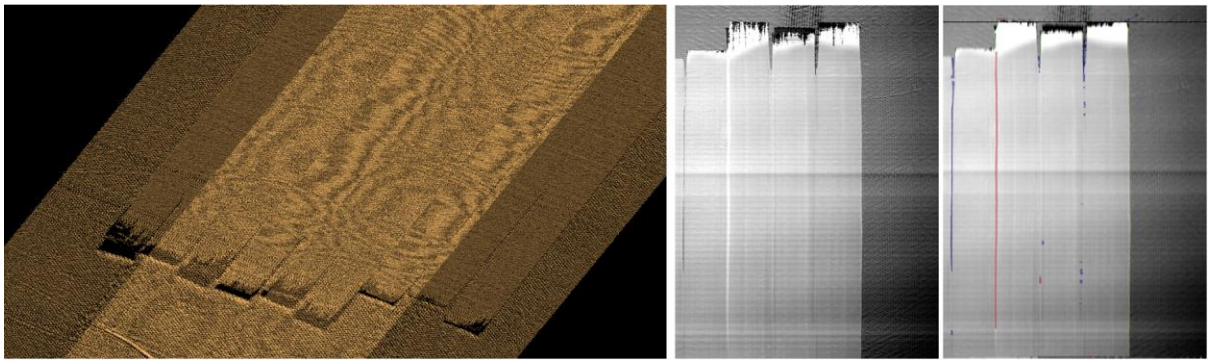

**Figure 9: 3D point cloud (left). Height profiles (middle). Evaluated height profiles (right).**

## 7. CONCLUSIONS

Usually performance of launcher components is decreased by dividing them into subcomponents due to additional interfaces. This is especially true for components with carbon fiber reinforcements. DLR developed a design that adds 50 mm of additional wall thickness only, while simplify manufacturing and systems installation. The shown manufacturing processes are feasible with a minimal set of robotic hardware, suited for small production volumes. Several challenges could be identified throughout this experiment: the scaling of tank resulted in narrow steering radii for the tape laying. To ensure manufacturability smaller tape widths should be used. However this may not be a problem in a full scale part where greater radii can be expected. As LM-PAEK prepreg tape and printable material are fairly new on the market their availability and quality are limited. For the tape this is noticeable in varying material quality and numerous splices. Printable LM-PAEK instead of PC would guarantee a

seamless transition between and tank and skirt and should be favored. The heating system was challenged with the continuous operation and xenon lamps show loss of performance with increasing wear. Nevertheless, the process showed potential to reduce part complexity by segmentation and joining of subparts. In-situ AFP showed good robustness with potential of further improvements using additional simulation and control capabilities. Further research may focus on reparability of a part that faces production errors in interaction with part design. At the same time solutions are required to increase crystallinity of large structures for example with an additionally annealing process step.

Finally, two inline quality assurance methods have been implemented and tested. The tape profile sensor system evaluated the tape position and could be used for on the flight correction of the robot in the future. Inline thermography has shown is capability to detect tape defects and trapped air, with direct correspondence to the tape position. The data generated during the thermography measurements could be used to develop an active thermography evaluation in the future. Therefore a hand eye calibration has to be performed to connect robot positions to camera positions and rectify the camera pictures. With rectified pictures, times, camera positions and robot velocity the pixels moving within each frame can be superimposed and Fourier transformed to generate phase and amplitude images of the complete measured track.

## 8. REFERENCES


[1] Achary, D., Biggs, R., Bouvier, C., McBain, M. and Lee, W. 2005. Composite Development and Applications for Cryogenic Tankage. *46th AIAA/ASME/ASCE/AHS/ASC Structures, Structural Dynamics and Materials Conference* (Apr. 2005).

[2] Aoki, T., Ishikawa, T. and Morino, Y. 2001. Overview of basic research activities on cryogenic composite propellant tanks in Japan. *10th AIAA/NAL-NASDA-ISAS International Space Planes and Hypersonic Systems and Technologies Conference* (Apr. 2001).

[3] Denkena, B., Schmidt, C., Völtzer, K. and Hocke, T. 2016. Thermographic online monitoring system for Automated Fiber Placement processes. *Composites Part B: Engineering*. 97, (Jul. 2016), 239–243.

[4] Krebs, F. 2018. Towards plug and work OPC UA as middleware of modern automation systems. *ISR 2018; 50th International Symposium on Robotics* (Jun. 2018), 1–6.

[5] Maldague, X. 2001. *Infrared and thermal testing*. American Society for Nondestructive Testing.

[6] McCarville, D.A., Guzman, J.C., Dillon, A.K., Jackson, J.R. and Birkland, J.O. 2018. 3.5 Design, Manufacture and Test of Cryotank Components. *Comprehensive Composite Materials II*. Elsevier. 153–179.

[7] Musk, E. 2018. Making Life Multi-Planetary. *New Space*. 6, 1 (Mar. 2018), 2–11.

[8] Palardy, G., Senders, F., Beurden, M. van and Villegas, I. 2017. Continuous ultrasonic welding of thermoplastic composite plates. *3rd International Symposium on Automated Composites Manufacturing* (Montreal, QC, Canada, 2017).

[9] RocketLab 2020. https://www.rocketlabusa.com/electron/, last accessed 2020-05-15.

[10] Sippel, M., Kopp, A., Mattsson, D., Freund, J., Tapeinos, I. and Koussios, S. 2015. Final Results of Advanced Cryo-TanksResearch Project CHATT. *6th European Conference for Aeronautics and Space Sciences* (2015).

[11] Tateishi, N., Zach, T.B., Woodhams, R.T. and North, T.H. 1989. Ultrasonic Bonding of Roll- drawn Polypropylene Using Tie-layers. *Proceedings of the 47th Annual Technical Conference (ANTEC'89)* (1989), 496–498.

[12] Yousefpour, A., Hojjati, M. and Immarigeon, J.-P. 2004. Fusion Bonding/Welding of Thermoplastic Composites. *Journal of Thermoplastic Composite Materials*. 17, 4 (Jul. 2004), 303–341.

[13] Zheng, H., Zeng, X., Zhang, J. and Sun, H. 2018. The Application of Carbon Fiber Composites in Cryotank. *Solidification*. InTech.